# Flood Susceptibility Mapping using Fuzzy Analytical Hierarchy Process for Cedar Rapids, Iowa

Beyza Atiye Cikmaz[1], Enes Yildirim[2], Ibrahim Demir[2,3]

[1] School of Urban and Regional Planning, University of Iowa, Iowa City, Iowa, US
[2] Department of Civil and Environmental Engineering, University of Iowa, Iowa City, Iowa, US
[3] Department of Electrical and Computer Engineering, University of Iowa, Iowa City, Iowa, US

Corresponding Author: Enes Yildirim, enes-yildirim@uiowa.edu

## Abstract

Floods affect over 2.2 billion people worldwide, and their frequency is increasing at an alarming rate compared to other natural disasters. Presidential disaster declarations have issued increasingly almost every year in Iowa for the past 30 years, indicating that the state is on the rise of flood risk. While significant scientific and technological advancement is becoming available for many flood mitigation activities, their on-the-ground consequences are hampered, among other things, by the lack of tools to quickly integrate the growing data into accessible and usable flood mitigation decisions. A multi-disciplinary approach is required, in which the underlying hydrologic processes that cause floods are closely linked with watershed-level socio-economic functions using effective collaboration tools to ensure community participation in the co-production of mitigation plans while paying attention to socio-environmental justice principles. Considering the existing limitations and needs, we conducted a flood risk assessment by utilizing geophysical and socio-economic datasets for a case study in Cedar Rapids, Iowa. Flood risk outputs are generated based on three main risk groups: geophysical-based flood risk, socioeconomic risk, and combined flood risk. Our results indicate that high- and very-high-risk flood susceptibility zones are primarily located in central urban areas with lower elevations. According to overall results, a large area of Cedar Rapids consists of a medium risk level according to the flood risk map combined with the fuzzy AHP method. The results show that high and very high-risk areas are 16% of the examined area, medium, low and very low-risk areas correspond to 84%. Besides, nearly 40% of the population lives in high to very high flood risk zones.

**Keywords:** Flood, Susceptibility Mapping, Hazard, Fuzzy Logic, AHP

*This manuscript is an EarthArXiv preprint and has been submitted for possible publication in the International Journal of Disaster Risk Reduction. Please note that* ***this has not been peer-reviewed before*** *and is* ***currently undergoing peer review for the first time****. Subsequent versions of this manuscript may have slightly different content. If accepted, the final version of this manuscript will be available via the 'Peer-reviewed publication DOI' link on this webpage. Please feel free to contact the authors; we welcome feedback.*

## 1. Introduction

Floods are occurring more frequently, and their magnitudes and impacts are increasing in many regions around the world. Flooding alone account for 75% of disaster-related fatalities across the globe (WHO, 2014). Natural disasters are projected to cost more than $300 billion per year in direct asset losses; this figure rises to $520 billion when indirect losses are taken into account (Hallegatte et al. 2017; Rentschler and Salhab, 2020). In addition to the economic losses, social insecurity, food security, and production distributions that are challenging to quantify but are undeniable consequences of natural hazards (Haltas et al., 2021; Yildirim and Demir, 2022a; World Bank, 2021). To mitigate the effects of these consequences on communities, decision-makers develop flood preparedness strategies and mitigation action plans in their jurisdictions (Teague et al., 2021; Yildirim, 2017). Due to the complexity of the flooding phenomena, socioeconomic and demographic factors (Tate et al., 2021a) and ethical considerations (Ewing and Demir, 2021) are essential along with geophysical parameters to consider in the decision-making process. By employing such interdisciplinary approaches, identifying at-risk regions and prioritizing mitigation resources can be successfully achieved (Tate et al., 2021b).

Recent studies highlight the potential benefits of an integrated flood risk management approach that not only covers the hydraulic/hydrologic modeling (Muste et al., 2017) point of view but also includes socioeconomic and demographic considerations (Thieken et al., 2013; Buchecker et al., 2016). An integrated approach embraces risk management measures, their feasibility, and effectiveness in a multidisciplinary context, including social, economic, and environmental aspects (Hall et al., 2003). In the literature, community engagement (Rogers et al., 2020), crop loss (Yildirim and Demir, 2022b), intelligent systems and demographics (Eryilmaz Turkkan and Hirca, 2021) are introduced as potential improvements that the interdisciplinary flood risk management framework can provide. Furthermore, the outcomes of such approaches can provide new insights into existing risks in communities as well as informative risk maps for planning and preparedness.

Flood risk and vulnerability assessments generate guiding maps for decision support such as potential transportation disruption (Alabbad et al., 2021), cost-benefit analysis (Yildirim and Demir, 2021), inundation extent (Li et al., 2022), and fragility of critical infrastructures (Yildirim and Demir, 2019). Therefore, better-informed decisions can be made and disaster action plans can be enhanced to protect against flood impacts. Moreover, water related hazards including water quality (Jones et al, 2018) and flood risk (Alabbad et al., 2022) are communicated through information systems to inform potential risks to the public. Depending on the data availability and the expertise, flood risk and vulnerability maps may be limited to projecting existing flood risk. While novel data driven techniques and remote sensing have been widely used for data generation (Gautam et al., 2022) and augmentation (Demiray et al., 2021), data availability is still a big challenge (Ebert-Uphoff et al., 2017) for many regions in the world. The maps are primarily developed using several methodologies based on hydraulics, socioeconomical aspects, social vulnerability, and ecology (Scheuer et al., 2011). Therefore, decision-making can be a challenging task to ensure an integrated flood risk management practice. Multi-criteria decision-making (MCDM) can facilitate a versatile view of the flood risk to support mitigation decisions. Demographic, socioeconomic, and geophysical properties can be combined to generate comprehensive flood risk outputs which can support mitigation planning. Information systems are critical for communicating water related hazards including droughts, water quality (Demir et al., 2009) and flooding with novel visuzalition and virtual reality technologies (Sermet and Demir, 2020).

Deciding between various risk-mitigation or protective measures often includes competing and conflicting criteria that requires the use of MCDM methodologies. One of the most widely utilized MCDM methodologies is the analytical hierarchy process (AHP) (Tesfamariam and Sadiq, 2006). The AHP is a structured multi-parameter analysis approach for organizing and analyzing complex decisions and presents an accurate method for quantifying the weights of decision criteria (Boroushaki & Malczewski, 2010). AHP has also been widely used for solving various water resources problems (Willet & Sharda, 1991), flood risk (Sinha et al., 2008) and flood damage (Chen & Wang, 2004) analysis. However, since AHP is based on the expert's opinion, it can lead to uncertainty and subjectivity in the process. In comparison to the AHP technique, the FAHP can reduce or even eliminate ambiguity and lack of clarity in complicated decision-making situations, as well as improve the accuracy of the estimate of the given circumstance (Kerkez et al., 2017). The fuzzy modification of the AHP allows decision-making under uncertainty where the imprecise factors and criteria are represented as fuzzy numbers. The FAHP method uses a fuzzy judgment matrix with fuzzy numbers rather than exact numerical values of the comparison ratios and derives crisp weights from consistent and inconsistent fuzzy comparison matrices, which eliminates the need for additional aggregation and ranking procedures (Mikhailov & Tsvetinov, 2004). The fuzzy AHP technique, like the AHP method, has recently been used in flood risk assessment (Parhizgar et al., 2017; Meshram et al., 2019; Talha et al., 2019; Ekmekçioğlu et al., 2020).

Flood risk mapping is often a challenging task to provide a comprehensive risk assessment by covering social, economic, and geophysical processes as a whole. Data availability, knowledge of modeling, and expertise in required technologies (i.e., GIS, database management) are also critical for decision-makers to conduct such analysis. Communities may not always have access to risk maps that require extensive resources computational and data resources. While data driven approaches proved to be useful for generating flood maps (Hu and Demir, 2021; Li and Demir, 2022) with limited data and resources, researchers often depend on regulatory maps for flood risk analysis. In the state of Iowa, the frequency of flooding events has grown over the last couple of decades. So, flood risk management has become a continuous process to eliminate fatalities and reduce financial losses. Assessing the present risk is necessary to prioritize vulnerable regions and take adequate mitigation measures. Iowa has extensive data resources for understanding flood risk. The dataset includes state-wide and community level flood map libraries, and data on demographics (i.e., population, income, age), transportation network, and geophysical properties (i.e., soil, DEM, drainage network, land use). These datasets can be utilized in multi-criteria decision-making processes like AHP and FAHP. The MCDM can be applied to the datasets by considering their relevance. For instance, geophysical parameters or social parameters can be evaluated in their groups, or they can be combined by employing weights that are determined in the literature. Thus, a detailed flood risk assessment can be implemented to get a complete picture of the flood risk in the state.

The flood impact (a.k.a. flood risk) is the result of the superposition of hazards (processes leading to high river levels), exposure (the elements at risk due to flooding) and vulnerability (susceptibility of natural, economic, and social elements at risk to being damaged when flooded). Irrespective of the hazard extent (i.e., small or extreme), floods are considered disastrous or non-disastrous based on their socio-economic damage (Merz et al., 2021). Damages from disastrous riverine floods include a wide range of direct and indirect impacts, monetary, intangible (e.g., loss of life), and ancillary disruptions in society and the environment (e.g., traffic re-routing, evacuations, homelessness, and landslides). While hazards are physical processes propagating through the landscape as described by hydrologic/hydraulic routing, exposure and vulnerability entail socioeconomic processes that can be counteracted by enhancing resilience. For the present context, we define resilience as the capacity of a flood and its components to anticipate, absorb, adapt, and recover from flood impacts through structural and non-structural measures (Lei et al., 2013; Proag, 2014; Kreibich et al., 2017; Zevenbergen et al., 2020; McClymont et al. 2020). Thus, resilience can be better understood and improved by studying the implications of exposure and vulnerability.

This study presents analyisis of the water-related risks by linking underlying geophysical properties with socioeconomic aspects. Digital elevation models (DEMs), soil properties, and drainage networks are among the geophysical features, while socioeconomic aspects include transportation networks, income levels, vulnerable age groups, and property ownership types. These underlying properties are used to map the flood risk in their groups and then combined to project the risk from geophysical and socioeconomic perspectives.

In the following sections, materials and methods are described in detail. The Analytic Hierarchy Process (AHP) and Fuzzy Analytic Hierarchy Process (FAHP) are explained with the parameter selections and justifications. Then, a case study is presented for the city of Cedar Rapids, Iowa. In the results sections, key findings and generated maps are shared. In the final, limitations and future work are discussed.

## 2. Materials and Methods

This research aims to outline geophysical-based flood risk and vulnerability maps in Cedar Rapids, Iowa, using the Analytical Hierarchy Process (AHP) and the Fuzzy Analytical Hierarchy Process (FAHP) method. In the following sections, we explained the details of the AHP and FAHP methods in our study.

### 2.1. Analytic Hierarchy Process (AHP)

The Analytic Hierarchy Process (AHP) was designed to solve complex problems with multiple criteria (Saaty, 1980). This method evaluates decisions using mathematical methods that consider the preferences of decision-makers or groups of people in a particular field based on selected factors. AHP resolves the conflict between practical demand and scientific decision-making and finds means to combine qualitative and quantitative analysis, resulting in an approach that is both efficient and effective in complex situations (Yang et al., 2018). The application of the AHP method can be summarized into five stages as follows: defining the problem and identifying the parameters; rating parameters based on the AHP scale; generate the pairwise comparison matrix; calculate the relative weights of each parameter; evaluation of the consistency ratio (CR) value.

Pairwise Comparison Matrix: The comparative matrix represents the relative importance of numerical values based on the AHP scale (Table 1). The following expression (Eq. 1) is used for constructing a pairwise matrix:

$$A = \begin{pmatrix} a_{11} & a_{12} & \cdots & a_{1n} \\ a_{21} & a_{22} & \cdots & a_{2n} \\ \vdots & \vdots & \ddots & \vdots \\ a_{n1} & a_{n2} & \cdots & a_{n1} \end{pmatrix} \quad \text{(Eq. 1)}$$

The equation compares two factors. If a factor value in the row has more weight than another factor in the column, the value should be assigned from 1 to 9. On the other hand, if a factor has less weight than another factor in the column, the value should be assigned from 1/2 to 1/9, and inherently, the cross parameters should be equal to 1. Following the interpretation of the scales shown in Table 1, comparison matrices were set off for both geophysical and vulnerability factors according to the order of importance of the parameters (Table 2 and 3).

Table 1. AHP and FAHP scales for creating pairwise comparison matrix (Putra et al., 2018)

| **Interpretation** | **AHP Scale** | **TFN Scale** | **Reciprocal TFN Scale** |
|---|---|---|---|
| Equally important | 1 | (1, 1, 1) | (1, 1, 1) |
| Equal to moderate | 2 | (0.5, 1, 1.5) | (0.67, 1, 2) |
| Moderately important | 3 | (1, 1.5, 2) | (0.5, 0.67, 1) |
| Moderate to important | 4 | (1.5, 2, 2.5) | (0.4, 0.5, 0.67) |
| Important | 5 | (2, 2.5, 3) | (0.33, 0.4, 0.5) |
| Important to high important | 6 | (2.5, 3, 3.5) | (0.28, 0.33, 0.4) |
| High important | 7 | (3, 3.5, 4) | (0.25, 0.28, 0.33) |
| High to extreme important | 8 | (3.5, 4, 4.5) | (0.22, 0.25, 0.28) |
| Extremely important | 9 | (4, 4.5, 4.5) | (0.22, 0.22, 0.25) |

Table 2. Pairwise comparison matrices for geophysical parameters in the AHP method

| **Geophysical Parameters** | **Landuse** | **Elevation** | **Soil Type** | **Slope** | **River Drainage Density** |
|---|---|---|---|---|---|
| **Landuse** | 1.00 | 0.50 | 0.50 | 1.00 | 0.50 |
| **Elevation** | 2.00 | 1.00 | 2.00 | 3.00 | 1.00 |
| **Soil Type** | 2.00 | 0.50 | 1.00 | 2.00 | 1.00 |
| **Slope** | 1.00 | 0.33 | 0.50 | 1.00 | 0.33 |
| **River Drainage Density** | 2.00 | 1.00 | 1.00 | 3.00 | 1.00 |
| *$\lambda max$ = 5.06; CI = 0.01; RI = 1.12; CR = 0.013* | | | | | |

Table 3. Pairwise comparison matrices for socioeconomic parameters in the AHP method

| **Vulnerability Parameters** | **Population** | **Income** | **Children & Elderly Pop.** | **Road Network Density** | **Renters** |
|---|---|---|---|---|---|
| **Population** | 1.00 | 5.00 | 2.00 | 1.00 | 3.00 |
| **Income** | 0.20 | 1.00 | 0.33 | 0.25 | 0.50 |
| **Children & Elderly Population** | 0.50 | 3.00 | 1.00 | 1.00 | 2.00 |
| **Road Network Density** | 1.00 | 4.00 | 1.00 | 1.00 | 2.00 |
| **Renters** | 0.33 | 2.00 | 0.50 | 0.50 | 1.00 |
| *$\lambda max$ = 5.04; CI = 0.01; RI = 1.12; CR = 0.008* | | | | | |

AHP weights of each parameter: After the creation of the pairwise matrix, the normalization of the matrix is required by applying Eq. 2 and Eq.3.

$$b_{ij} = \frac{a_i}{\sum_{i=1}^{n} a_{ij}} \quad \text{(Eq. 2)}$$

$$A = \begin{pmatrix} b_{11} & b_{12} & \cdots & b_{1n} \\ b_{21} & b_{22} & \cdots & b_{2n} \\ b_{n1} & b_{n2} & \cdots & b_{nm} \end{pmatrix} \quad \text{(Eq. 3)}$$

To find the weight of each parameter, the average of each row is estimated in the normalized pairwise comparison matrix using Equation 4.

$W_i = \frac{\sum_{j=1}^{n} b_{ij}}{n}$ and $\sum_{i=1}^{n} W_i = 1$ (Eq. 4)

where "n" represents the number of factors.

Consistency Evaluation: The consistency ratio (CR) is calculated to verify the consistency of the comparisons. If the value of CI is zero, the matrix is considered consistent (Putra et al., 2018). Moreover, if CR is less than 0.1, there is a reasonable level of consistency in the pairwise comparison matrix, whereas CR is more than 0.1 implies inconsistent assessments. The CR value is the product of the CR value over the RI value which is shown in Equation 5 and 6.

$$CI = \frac{\lambda max - n}{n-1} \quad \text{(Eq. 5)}$$

$$CR = \frac{\text{Consistency Index (CI)}}{\text{Random Index (RI)}} \quad \text{(Eq. 6)}$$

where, λmax is the largest Eigenvalue obtained from the pairwise matrix, and n is the number of parameters (Malczewski, 1999). Also, RI represents the random index which is dependent on the size of the matrix (Table 4), and the 1.12 value was chosen for RI because of our number of parameters.

Table 4. Random Index (RI) (Saaty, 1980)

| **n** | **1** | **2** | **3** | **4** | **5** | **6** | **7** | **8** | **9** |
|---|---|---|---|---|---|---|---|---|---|
| **RI** | 0 | 0 | 0.58 | 0.90 | 1.12 | 1.24 | 1.32 | 1.41 | 1.45 |

### 2.2. Fuzzy Analytic Hierarchy Process (FAHP)

In the AHP method, the value assigned for each param eter cannot be accurately represented with crisp numbers since it is a result of human judgments and preferences. Therefore, fuzzy set theory can address this ambiguity and uncertainty issue and calculate human judgments with the least number of errors (Zadeh, 1965; Ahmed et al., 2018). Several FAHP methodologies have been introduced over the past couple of decades (Van Laarhoven and Pedrycz, 1983; Buckley, 1985; Chang, 1996). Fuzzy Extent Analysis , one of the FAHP methods prepared by Chang (1996), is suggested to be more suitable, particularly for the risk assessment applications (Radionovs & Uzhga-Rebrov, 2017). We identified flood susceptibility areas using this approach, and then following stages are applied: Stage 1: Creation of Fuzzy Judgment Matrix; Stage 2: Calculation of the fuzzy synthetic extent value (*Si*); Stage 3: Computation of the magnitude of *Si*; Stage 4: Calculation of the weight of each factor; Stage 5: Normalization of the final weight factor.

Fuzzy Judgment Matrix: It is combined with the pairwise comparison matrix and triangular fuzzy number (TFN) of fuzzy set theory. The TFN is represented as l, m, and u where they stand for the lowest value, the middle value, and the upper value of a fuzzy set, respectively. The transformation of AHP to FAHP measures is given in Table 1 and the fuzzy judgment matrices of the 10 parameters employed can be seen in Table 5 and 6. After the identification of the triangular fuzzy numbers, the fuzzy judgment matrix is created as follows:

$$\tilde{A} = \begin{bmatrix} \breve{1} & \breve{a}_{12} & \cdots & \breve{a}_{1n} \\ \breve{a}_{21} & \breve{1} & \cdots & \breve{a}_{2n} \\ \cdots & \cdots & \breve{1} & \cdots \\ \breve{a}_{n1} & \breve{a}_{n2} & \cdots & \breve{1} \end{bmatrix} \quad \text{(Eq. 7)}$$

Table 5. Fuzzy judgment matrices for geophysical parameters in the FAHP method

| Geophysical Parameters | Landuse | Elevation | Soil Type | Slope | River Drainage Density |
|---|---|---|---|---|---|
| **Landuse** | (1, 1, 1) | (0.67, 1, 2) | (0.67, 1, 2) | (1, 1, 1) | (0.67, 1, 2) |
| **Elevation** | (0.5, 1, 1.5) | (1, 1, 1) | (0.5, 1, 1.5) | (1, 1.5, 2) | (1, 1, 1) |
| **Soil Type** | (0.5, 1, 1.5) | (0.67, 1, 2) | (1, 1, 1) | (0.5, 1, 1.5) | (1, 1, 1) |
| **Slope** | (1, 1, 1) | (0.5, 0.67, 1) | (0.67, 1, 2) | (1, 1, 1) | (0.5, 0.67, 1) |
| **River Drainage Density** | (0.5, 1, 1.5) | (1, 1, 1) | (1, 1, 1) | (1, 1.5, 2) | (1, 1, 1) |

Table 6. Fuzzy judgment matrices for socioeconomic parameters in the FAHP method

| Vulnerability Parameters | Population | Income | Children & Elderly Pop. | Road Network Density | Renters |
|---|---|---|---|---|---|
| **Population** | (1, 1, 1) | (2, 2.5, 3) | (0.5, 1, 1.5) | (1, 1, 1) | (1, 1.5, 2) |
| **Income** | (0.33, 0.4, 0.5) | (1, 1, 1) | (0.5, 0.67, 1) | (0.4, 0.5, 0.67) | (0.67, 1, 2) |
| **Children & Elderly Population** | (0.67, 1, 2) | (1, 1.5, 2) | (1, 1, 1) | (1, 1, 1) | (0.5, 1, 1.5) |
| **Road Network Density** | (1, 1, 1) | (1.5, 2, 2.5) | (1, 1, 1) | (1, 1, 1) | (0.5, 1, 1.5) |
| **Renters** | (0.5, 0.67, 1) | (0.5, 1, 1.5) | (0.67, 1, 2) | (0.67, 1, 2) | (1, 1, 1) |

Fuzzy Synthetic Extent Value ($S_i$): Si that is computed in equation 8 for each row of the fuzzy judgment matrix can be used as:

$$S_i = \sum_{j=1}^{m} M_{gi}^{j} \times \left[ \sum_{i=1}^{n} \sum_{j=1}^{m} M_{gi}^{j} \right]^{-1} \quad \text{(Eq. 8)}$$

$$\sum_{j=1}^{m} M_{gi}^{j} = \left( \sum_{j=1}^{m} l_i \sum_{j=1}^{m} m_i \sum_{j=1}^{m} u_i \right) \quad \text{(Eq. 9)}$$

$$\left[ \sum_{i=1}^{n} \sum_{j=1}^{m} M_{gi}^{j} \right]^{-1} = \left( \frac{1}{\sum_{i=1}^{n} u_i}, \frac{1}{\sum_{i=1}^{n} m_i}, \frac{1}{\sum_{i=1}^{n} l_i} \right) \quad \text{(Eq. 10)}$$

where *i* denote the row number, while *j* represents the column number.

Computation of the Magnitude of $S_i$ : $S_1 = (l_1; m_1; u_1)$ and $S_2 = (l_2; m_2; u_2)$, where $S_1 \geq S_2$ can be expressed in Eq. 11.

$$V\ (S_1 \geq S_2)$$

$$V = \left\{ \begin{array}{lll} 1 & if & m_1 \geq m_2 \\ 0 & if & l_2 \geq u_1 \\ \frac{l_2 - u_1}{(m_1 - u_1) - (m_2 - l_2)} & & otherwise \end{array} \right\} \quad \text{(Eq. 11)}$$

FAHP weights of each parameter: Eq. 12 is used to calculate the magnitude of a convex fuzzy number derived from "k" as another degree of possibility of fuzzy number:

$$V\ (S \geq S_1, S_2, \dots S_k) = V\ (S \geq S_1)\ and\ (S \geq S_2)\ and \dots and (S \geq S_k)$$

$$V = \min\ V\ (S \geq S_i),\ \ i = 1, 2, \ldots, k \tag{Eq. 12}$$

To find the weight of factors ($W'$), Eq. 13 and Eq. 14 can be utilized.

$$d'(A_i) = \min V(S_i \geq S_k), for\ k = 1, 2, \ldots, n; k \neq i \tag{Eq. 13}$$

$$W' = (d'(A_1), d'(A_2), \ldots, d'(A_n)) \tag{Eq. 14}$$

Normalization of the final weight factor: At the last stage, the final parameter weights are normalized to obtain the non-fuzzy number as shown in Eq. 15.

$$W\ (A_i) = \frac{d'(A_i)}{\sum W'} \tag{Eq. 15}$$

**2.3. Cedar Rapids Case Study**

Cedar Rapids, which is located in eastern Iowa, was selected as the study site. The Cedar Rapids is the second-largest city in the state, with a population of 137,710 (U.S. Census Bureau, 2021). The elevation is between 213 m and 270 m. Agriculture and agriculture-related industries are the main economic activities in the city. Particularly in the upstream region, agriculture is intensively practiced by using tile drainage systems that are found to be one of the contributing factors to flood events (Thomas, 2015). The Cedar River is the major stream passing through the city center and repeatedly causes flooding events (e.g., 2008, 2014, 2016, 2019). The city was significantly affected by the June 2008 flood, as reflected in the federally supported program with the acquisition of over 1300 damaged properties. The flooded areas of this event overlapped with the majority of the affordable housing blocks within the city, leaving their residents exposed to deepening poverty, marginalization, and exclusion (Tate et al., 2016). In this research, we identified a grid shown in Figure 1 to collect and analyze the available datasets for the city. An extensive dataset including demographic, economic, soil, and geographic data was collected for Cedar Rapids.

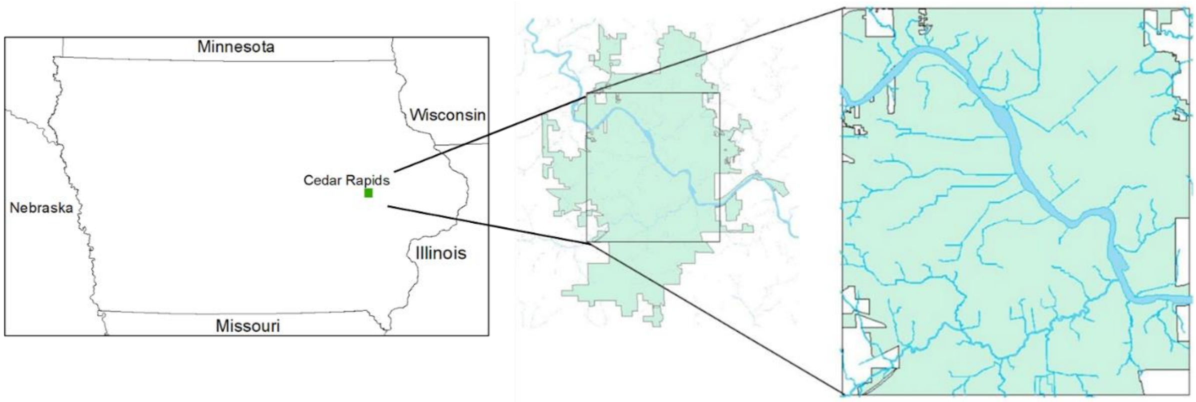


Figure 1. Case study maps of the Cedar Rapids with Iowa and specific focused region

**2.4. Parameter Selection and Data Processing**

Each risk variable differs from region to region; in other words, an indicator that significantly impacts the flood risk in a particular area may not always show the same value in another area (Wang et al., 2020). In this study, a total of 10 parameters were selected. Out of the ten parameters, there are five geophysical (G) and five vulnerability (V) indicators. Data sources and detailed descriptions of each parameter are shown in Table 7.

Table 7. Data sources and resolution of parameters

| Data/Parameters | Resolution | Data Sources |
|---|---|---|
| Elevation (G) | 30 x 30 m | Iowa Department of Natural Resources (Iowa DNR, 2021a) |
| River Drainage Density (G) | 5 x 5 m | Generated using the river network data (Demir and Szczepanek, 2017) |
| Soil Type (G) | 10 x 10 m | United States Department of Agriculture, Soil Survey Geographic Database (USDA, 2021) |
| Land use (G) | 30 x 30 m | United States Department of Agriculture, CropScape and Cropland Data Layer (NASS,2021) |
| Slope (G) | 5 x 5 m | Generated using DEM |
| Population (V) | Census Block | Federal Emergency Management Agency, HAZUS Database (FEMA, 2021) |
| Road Network Density (V) | 5 x 5 m | Generated using the transportation network |
| Children & Elderly Population (V) | Census Block | Federal Emergency Management Agency, HAZUS Database (FEMA, 2021) |
| Renters (V) | Census Block | Federal Emergency Management Agency, HAZUS Database (FEMA, 2021) |
| Income Rating (V) | Census Block | Federal Emergency Management Agency, HAZUS Database (FEMA, 2021) |
| River Network | Vector Data | Iowa Department of Natural Resources (Iowa DNR, 2021b) |
| Transportation Network | Vector Data | OpenStreetMap Vector Layers (OpenStreetMap, 2021) |

A detailed description of geophysical and vulnerability parameters are as follows:

**Elevation (G):** Elevation is found as the dominant factor that has a great impact on flooding (Mojaddadi et al., 2017; Bouamrane et al., 2020). Generally, flood hazards are more likely to be found in low altitudes rather than high altitudes.

**River Drainage Density (G):** Riverbanks are high-risk areas for flooding; hence, distance from rivers can be a determining factor in flooding (Eini et al., 2020). River drainage density was calculated from the river vector data of the region using the linear density analysis in ArcGIS. High-density areas will be more vulnerable to flood, and low-density areas are considered low-risk areas.

**Soil Type (G):** Each soil type has unique water holding capacities and this information can be used to understand the surface runoff rate. Soil types were classified into five classes based on plant-available water holding capacity (UC Drought Management, 2021).

**Land use (G):** Land-use influences infiltration, evapotranspiration, and runoff processes; therefore, it considerably impacts a river basin's hydrological cycle (Bouamrane, 2020). Like soil type, land use pattern significantly impacts water permeability capacity. For instance, water permeability is low in urban areas, while permeability rate is high in forest and vegetation-covered areas.

**Slope (G):** In hydrological studies, terrain slope has a significant role in regulating surface discharge (Das, 2019). It was generated by using the elevation data in QGIS. It provides topographic change and runoff velocity. Steep slopes increase the rate of water flow, but flooding usually occurs in flat or gently sloped areas.

**Population (V):** One of the most important variables in evaluating social vulnerability is the population (Dandapat & Panda, 2017). Therefore, the indicator of the population was given the highest importance among other vulnerability parameters. This data was extracted from US census data in 2010. In Figure 2, population distribution is given for the study site.

**Road Network Density (V):** Transportation network data is processed to create road network density using the same technique that drainage density data was created. In the floodplain, roads are prone to damage, and transportation interruptions in intracity and interurban transport are possible. So, it is considered that the greater the density of roads, the greater the capacity of people to cope with floods (Duan et al., 2021).

**Children and Elderly (V):** Due to various physiological reasons arising from their age, children (0-16 years old) and the elderly (65 years and above) are particularly susceptible to flooding (Wang et al., 2020a).

**Renters (V):** Reasons such as lack of control over home repairs and limited insurance indicate that renters are more vulnerable than homeowners (Rufat et al., 2015).

**Income Rating (V):** It refers to the socio-economic situation for each census level. According to Wang et al. (2020b), high-income rating areas represent more resilience for pre-and post-disaster.

All parameters were resampled to a 5 by 5-meter grid data layer using ArcGIS to the same grid. After the data resampling, each layer was divided into five flood risk classes, as 1 is very low, 2 is low, 3 is middle, 4 is high, and 5 is a very high risk, as demonstrated in Table 8. Since different indicators exhibit contributions differently to flood risk, weights of AHP were used for parameters to produce geophysical-based risk maps and vulnerability maps. Then, these two maps have been combined with the weight of %50 for each to generate a combined flood risk map. After that, the same method was followed, with the only difference being that FAHP weights were used instead of AHP weights. A total of 6 maps were produced, three of them were created using AHP, and the remaining maps using the FAHP method. The adopted methodology in the study is briefly summarized in Figure 3.

Table 8. Classification of geophysical and vulnerability parameters

| **Parameters** | | **Unit** | **Parameter Classes** | | | | |
|---|---|---|---|---|---|---|---|
| | | | **1** | **2** | **3** | **4** | **5** |
| **Geophysical** | Elevation (m) | meter | 269-284 | 254-269 | 239-254 | 224-239 | 209-224 |
| | River Drainage Density | km / $km^2$ | 0-2.5 | 2.5-5 | 5-7.5 | 7.5-10 | >10 |
| | Soil Type | -- | clay loam, silty clay loam | silt loam, loam | sandy loam, complex, others | urban land complex | water bodies |
| | Land use | -- | wetland | open space, forest | agricultural crop land, vegetation | built-up area | water bodies |
| | Slope | degree | >15 | 8-15 | 4-8 | 2-4 | 0-2 |
| **Vulnerability** | Population | -- | 0-50 | 50-200 | 200-350 | 350-500 | 500-1132 |
| | Road Network Density | km / $km^2$ | 0-3 | 3-6 | 6-9 | 9-12 | 12-24 |
| | Children & Elderly Population | -- | 0-5 | 5-50 | 50-100 | 100-200 | 200-449 |
| | Renters | -- | 0-1 | 1-100 | 100-200 | 200-300 | 300-1100 |
| | Income Rating | -- | 1,618-2,670 | 1,171-1,618 | 892-1,171 | 608-892 | 281-608 |

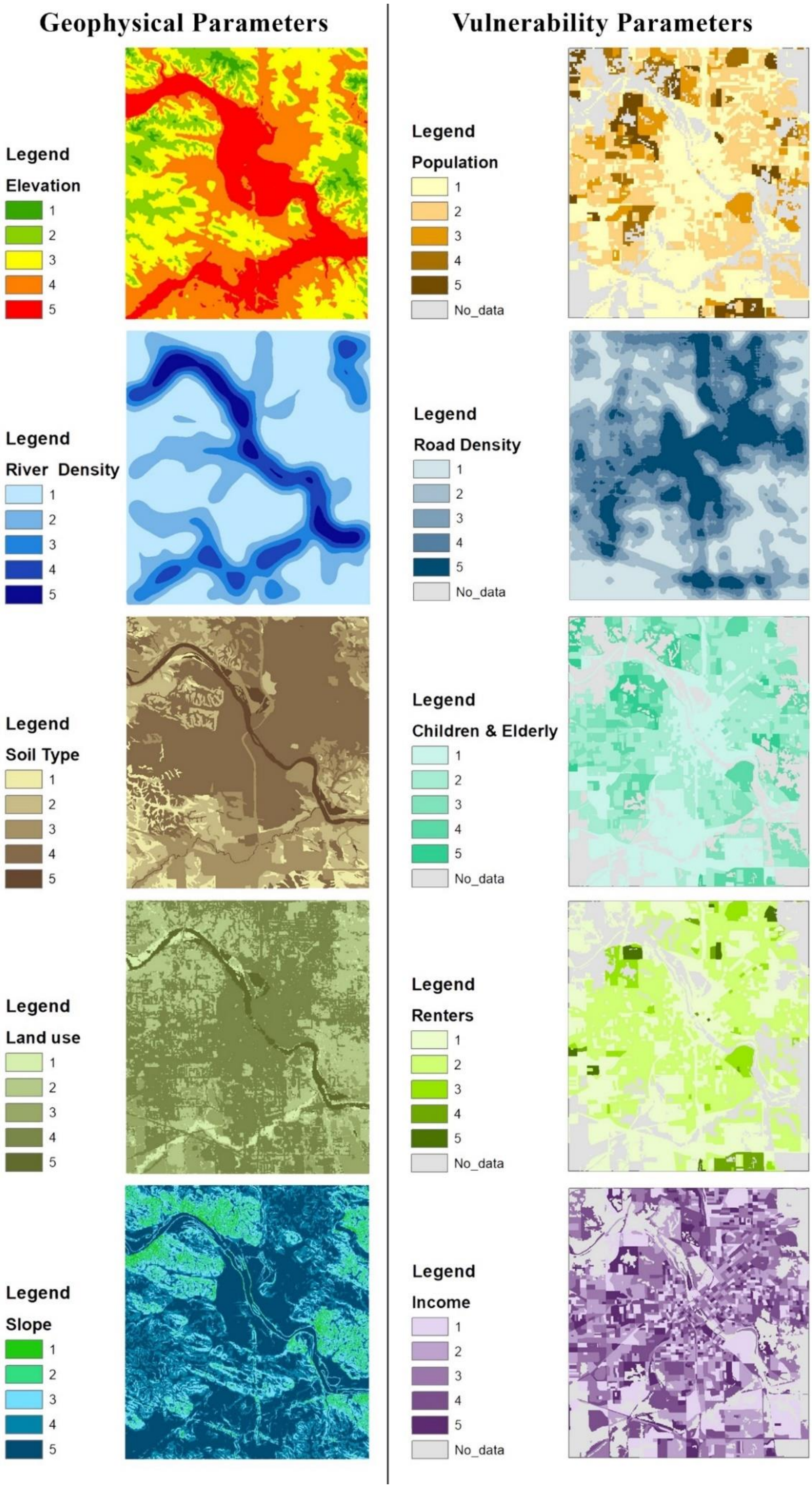


Figure 2. Spatial distribution of geophysical and vulnerability parameter classes

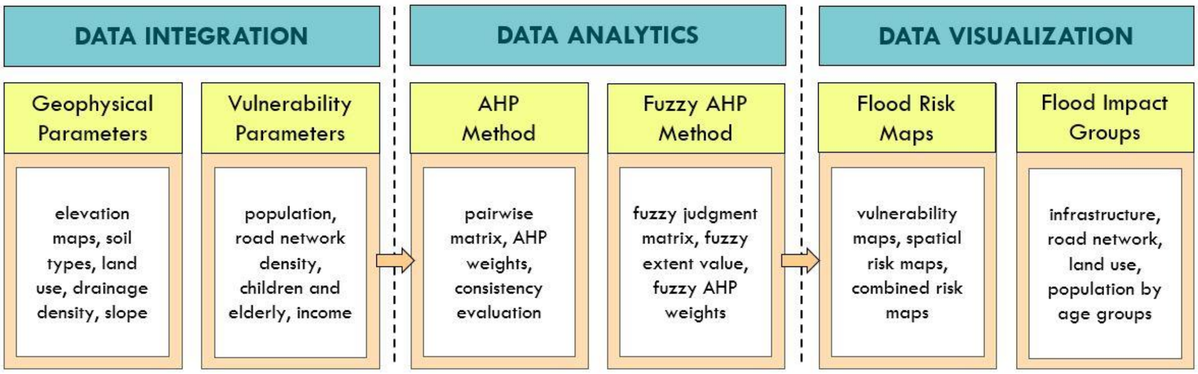


Figure 3. Schema and components of the methodology

## 3. Results and Discussion

### 3.1. AHP and FAHP Comparison

The AHP model was primarily used to calculate each parameter to verify the consistency ratio since the approach is based on expert judgment in determining the relative importance of physical and demographic factors. After the verification, the final weight factor was calculated for AHP and FAHP (refer to Table 9). For geophysical factors based on AHP, the relative weight of elevation is the highest, with a value of 0.30, followed by the river drainage density and soil type with a value of 0.26 and 0.21, respectively. Land use and slope were considered less influencing compared with the previous factors with weight values of 0.12 and 0.10 respectively. Meanwhile, for vulnerability factors using the same method, the highest impacting factor is the population with 0.34, and the density of the road network and the population of children and elderly were followed by 0.26 and 0.21. Renters and income rating factors had lower importance with weights of 0.12 and 0.07, respectively. In the FAHP model, the most important flood conditioning factors were elevation, river drainage density, soil type, and land use with weights of 0.22, 0.21, 0.20, and 0.20, respectively, whereas slope had the lowest weight of 0.17 in geophysical parameters. Similar to AHP, the population was the highest with 0.26 compared to the other vulnerability factors, followed by road network density and children and elderly population with weight values of 0.22 and 0.20, while renters and income rating had low degrees of importance with weights of 0.18 and 0.14 respectively. Consequently, the weight ranking of factors was almost the same in both methods. The only difference was the soil type and land use weights which were the same in the FAHP method. In the FAHP, it is also noticeable that the weight values are closer to each other for each parameter.

Table 9. Weights of geophysical and vulnerability parameters used in AHP and FAHP

| **Parameter** | **AHP Weight** | **FAHP Weight** |
|---|---|---|
| Elevation | 0.30 | 0.22 |
| River Drainage Density | 0.26 | 0.21 |
| Soil Type | 0.21 | 0.20 |
| Land use | 0.12 | 0.20 |
| Slope | 0.10 | 0.17 |
| Population | 0.34 | 0.26 |
| Road Network Density | 0.26 | 0.22 |
| Children & Elderly Population | 0.21 | 0.20 |
| Renters | 0.12 | 0.18 |
| Income Rating | 0.07 | 0.14 |

### 3.2. Spatial Distribution of Flood Risk in Cedar Rapids

Based on the weights from both methods, the spatial distribution of geophysical-based flood risk and vulnerability maps was generated for Cedar Rapids at a 5-meter resolution. Five geophysical and five vulnerability factors were analyzed within their groups by using the determined weights. Then, the geophysical and vulnerability maps were combined using the AHP and FAHP weights. When combined flood risk maps were created, 50% weights were applied to both groups. Finally, a total of six analysis were carried out and maps were generated. The final maps were classified into five flood susceptibility classes: very low, low, moderate, high, and very high. However, very low class was not attained in both combined maps after merging the geophysical and vulnerability maps.

In general, high- and very-high-risk flood susceptibility zones are roughly centered on the downtown areas, which have lower elevations and are close to the city center. In geophysical based flood risk maps, high and very high-risk areas are found in water bodies and around the water resources, and these high and very-high risk areas cover about 25% and 35% of the area, AHP and FAHP, respectively (see Figure 4). Unlike geophysical maps, we observed that the high-risk areas are far from the water sources where the population and road density values are high in vulnerability maps. The high-risk zones (4 and 5 classes) constitute 7% in AHP, 6% in FAHP method of the studied area. Besides, very high-risk and high-risk areas are mainly located in the research area's central, northwestern, and southeastern zones, accounting for approximately 11% and 16% of the total area in the AHP and FAHP combined flood risk map, respectively.

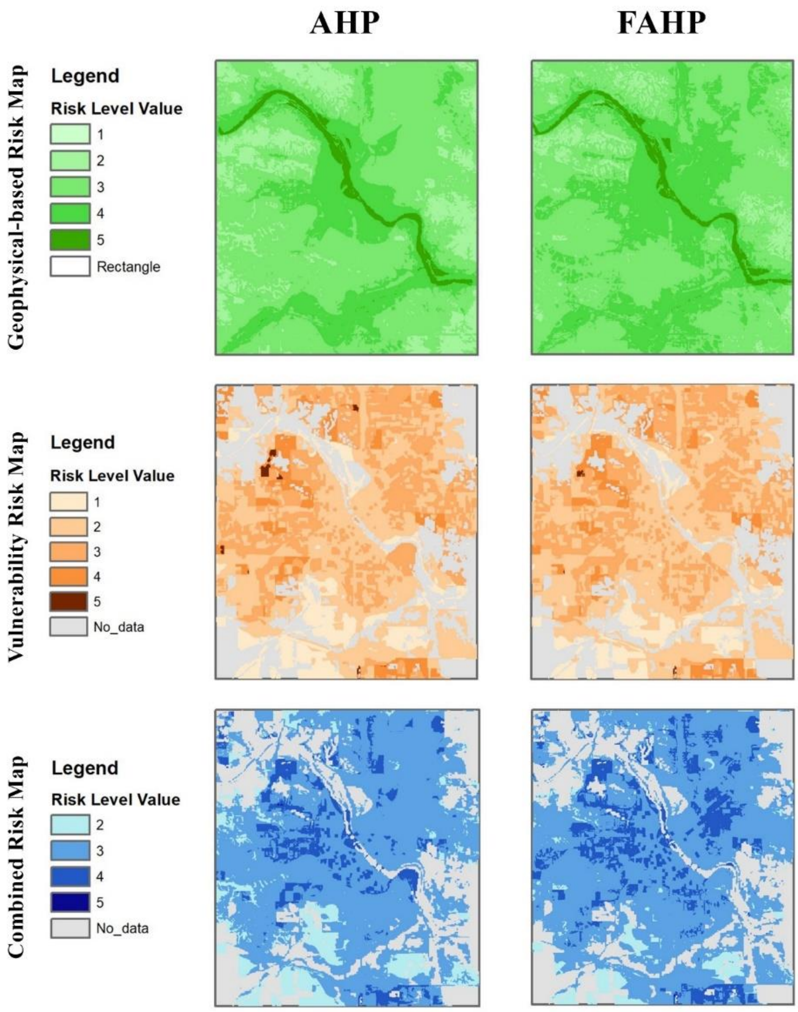


Figure 4. Flood risk maps based on the AHP and FAHP methods

The spatial distribution of flood risk maps enables decision-makers to clearly identify risk areas. Since the flood risk in an area is the result of the interaction of geophysical and socioeconomic factors, flood risk maps should be considered geophysical or vulnerability parameters alone are neither integrated nor objective. Geophysical parameters indicate the regions where a flood can likely or unlikely propagate, while flood vulnerability parameters represent susceptibility to damage and the risk for human lives. The spatial distribution of the combined flood risk and geophysical-based maps had similar trends, yet the mismatches were apparent in certain zones that are significantly affected by socioeconomic factors. There are some areas with low hazard intensity that might also have a high flood risk. For instance, the areas in the southeast and northeast of the study area are the high and very high-risk zones due to their dense populations, transportation, number of children, and elderly, but these areas had moderate or low risk according to the geophysical-based risk map.

### 3.3. Flood Risk Quantification for Geophysical and Vulnerability

Demographic and socioeconomic factors are critical inputs to understand the flood vulnerability in communities. Flood susceptibility zone maps and distinct thematic content maps can provide critical information regarding the risk of flooding in Cedar Rapids. Thus, structures, road types, land use, and population census data from 2010 were intersected with the obtained maps by using GIS technology, and statistical analysis was carried out in this study. Table 10 infers the percentages of structures, road types, land use, and population in five different risk classes on six maps produced using both methods.

Table 10 shows that the percentages of very low, low, and medium risk areas are higher in the AHP method than in the fuzzy method. In contrast, the percentages in the high and very high zones are higher in the fuzzy method. Moreover, moderate risk has the highest percentage of all variable types. The results evidently show that in high-risk areas at levels 4 and 5, in combined maps using the AHP and fuzzy method, the population has the highest percentage, with nearly 40%, while land use is the lowest, with about 11% in AHP and 16% in FAHP. Similarly, for the same areas in vulnerability maps, the population has a maximum risk of approximately 18% and 13% according to the AHP and FAHP methods, respectively, but the percentage of roads is the minimum risk at nearly 6% for both methods. Contrary to vulnerability maps, in geophysical-based risk maps, roads have the highest rate, while the population has the lowest rate. In geophysical-based maps, roads have the highest rate of high risk, accounting for almost 27% in AHP and 42% in FAHP, whereas the population has the lowest rate at 19% and 28%, respectively.

A detailed study was conducted by referring to the variables used in this study. The results of structure, road, and land use data were obtained based on the geophysical-based risk maps. Meanwhile, the population information was analyzed using vulnerability maps. Table 11, 12, 13 and 14 show the proportions of the exposed infrastructure, land use, and age groups in the high-risk flooding hazard zones. FAHP tends to estimate higher exposure compared to AHP. With the fuzzy method, it was determined that more than half of the commercial, medical and education buildings were located in high and very-high risk areas. When the total percentage was considered, the most vulnerable buildings were residential with over 34%. According to FAHP, the highest share in the relative percentage is secondary road, and in total percentage is residential road type. The methods we used in our assessment of flood risk can be proven to be valid through land-use types because it has been revealed that the uses with the utmost risk of almost 99 percent flooding have water resources. Besides, the area with the greater risk in the general percentage is the built environment, and the most at-risk age group here is adults who are between 16 and 65 years old.

Table 10. Distribution of variables based on flood risk levels

| | Risk Class | Combined Map (%) | | Geophysical Map (%) | | Vulnerability Map (%) | |
|---|---|---|---|---|---|---|---|
| | | AHP | FAHP | AHP | FAHP | AHP | FAHP |
| Structures | 1 | 0.0 | 0.0 | 0.0 | 0.0 | 0.8 | 0.7 |
| | 2 | 4.1 | 1.2 | 11.7 | 3.8 | 38.3 | 41.4 |
| | 3 | 80.0 | 71.1 | 69.2 | 57.0 | 51.8 | 49.8 |
| | 4 | 15.9 | 27.7 | 18.9 | 39.0 | 8.5 | 8.0 |
| | 5 | 0.0 | 0.0 | 0.2 | 0.2 | 0.6 | 0.1 |
| Road Types | 1 | 0.0 | 0.0 | 0.0 | 0.0 | 4.7 | 10.6 |
| | 2 | 6.3 | 12.4 | 10.3 | 6.6 | 50.4 | 47.2 |
| | 3 | 82.1 | 61.8 | 62.8 | 50.2 | 38.6 | 36.3 |
| | 4 | 11.6 | 25.7 | 26.0 | 41.5 | 5.9 | 5.6 |
| | 5 | 0.0 | 0.1 | 0.9 | 1.7 | 0.4 | 0.3 |
| Land Use | 1 | 0.0 | 0.0 | 0.0 | 0.0 | 13.3 | 10.4 |
| | 2 | 13.1 | 6.5 | 15.9 | 7.5 | 46.8 | 51.1 |
| | 3 | 76.0 | 77.4 | 58.6 | 57.3 | 32.5 | 32.4 |
| | 4 | 10.9 | 16.0 | 22.2 | 31.9 | 7.0 | 6.0 |
| | 5 | 0.0 | 0.1 | 3.3 | 3.3 | 0.4 | 0.1 |
| Population | 1 | 0.0 | 0.0 | 0.4 | 0.0 | 4.2 | 5.2 |
| | 2 | 20.0 | 13.4 | 33.0 | 36.1 | 35.3 | 37.8 |
| | 3 | 40.2 | 47.3 | 47.3 | 36.1 | 42.5 | 44.1 |
| | 4 | 38.9 | 38.5 | 18.7 | 27.2 | 15.5 | 11.6 |
| | 5 | 0.9 | 0.8 | 0.6 | 0.6 | 2.5 | 1.3 |

Table 11. Distribution of structure types in relation to geophysical and vulnerability maps

| Structure Types | Number of structures | Percentage within structures | High and very high zones | | | |
|---|---|---|---|---|---|---|
| | | | Relative percentage | | Total percentage | |
| | | | AHP | FAHP | AHP | FAHP |
| Residential | 31,311 | 90.6 | 17.46 | 37.62 | 15.81 | 34.07 |
| Commercial | 1,697 | 4.9 | 33.53 | 53.39 | 1.65 | 2.62 |
| Medical | 195 | 0.6 | 26.15 | 68.72 | 0.15 | 0.39 |
| Industry | 599 | 1.7 | 33.06 | 49.25 | 0.57 | 0.85 |
| Agriculture | 95 | 0.3 | 27.37 | 36.84 | 0.08 | 0.10 |
| Education | 63 | 0.1 | 28.57 | 50.79 | 0.05 | 0.09 |
| Others | 615 | 1.8 | 42.11 | 58.54 | 0.75 | 1.04 |

Table 12. Distribution of road types in relation to geophysical and vulnerability maps

| Road Types | Total km of roads | Percentage within road types | High and very high zones | | | |
|---|---|---|---|---|---|---|
| | | | Relative Percentage | | Total percentage | |
| | | | AHP | FAHP | AHP | FAHP |
| Motorway, Trunk | 77.2 | 9.3 | 29.75 | 38.02 | 2.75 | 5.32 |
| Primary | 39.0 | 4.7 | 17.47 | 46.59 | 0.82 | 2.75 |
| Secondary | 86.9 | 10.4 | 41.41 | 56.53 | 4.31 | 5.38 |

| | | | | | | |
|---|---|---|---|---|---|---|
| Tertiary | 81.8 | 9.8 | 22.99 | 44.47 | 2.26 | 4.63 |
| Residential | 535.4 | 64.1 | 22.35 | 41.22 | 14.34 | 23.73 |
| Others | 14.1 | 1.7 | 42.75 | 54.36 | 0.73 | 1.41 |

Table 13. Distribution of land use types in relation to geophysical and vulnerability maps

| **Land Use Types** | **Total km$^2$ of areas** | **Percentage within land use types** | **High and very high zones** | | | |
|---|---|---|---|---|---|---|
| | | | **Relative Percentage** | | **Total percentage** | |
| | | | **AHP** | **FAHP** | **AHP** | **FAHP** |
| Agricultural Land | 5.16 | 4.6 | 11.27 | 12.54 | 0.51 | 0.57 |
| Built-up Area | 60.02 | 52.9 | 28.49 | 48.69 | 15.7 | 25.77 |
| Forest | 12.32 | 10.9 | 10.74 | 8.95 | 1.17 | 0.97 |
| Open Space | 23.39 | 20.6 | 9.17 | 8.80 | 1.89 | 1.82 |
| Vegetation Cover | 4.57 | 4.0 | 20.10 | 22.52 | 0.81 | 0.91 |
| Water Bodies | 4.01 | 3.5 | 99.39 | 99.58 | 3.52 | 3.52 |
| Wetland | 3.92 | 3.5 | 73.30 | 48.83 | 2.54 | 1.69 |

Table 14. Distribution of population groups in relation to geophysical and vulnerability maps

| **Population based on ages** | **Number of people** | **Percentage within population** | **High and very high zones** | | | |
|---|---|---|---|---|---|---|
| | | | **Relative Percentage** | | **Total percentage** | |
| | | | **AHP** | **FAHP** | **AHP** | **FAHP** |
| Less 16 years | 29,646 | 23.4 | 18.19 | 12.39 | 4.16 | 2.78 |
| 16 to 65 years | 80,108 | 63.4 | 18.75 | 13.38 | 12.03 | 8.63 |
| Over 65 years | 16,572 | 13.2 | 14.25 | 11.26 | 1.85 | 1.46 |

## 4. Conclusion

Comprehensive flood risk analysis is essential for disaster planning, preparedness, and mitigation decisions. The outcome of these analysis can be improved by including physical and demographic data for a better understanding of potential implications. In this research, AHP and FAHP methods were carried out to identify and assess flood-prone areas in Cedar Rapids, Iowa. Numerous geophysical and vulnerability parameters that play a crucial role in flood risk assessment are employed in this study. Elevation, river drainage density, soil type, land use, slope, population, road network density, children and elderly population, renters, and income were assessed using MCDP. Flood risk maps were created using methods, and several parameters were generated for geophysical, vulnerability and combined flood risk. The spatial distribution of flood risk levels in the area was generated with a high resolution grid (5 m). As a final step, to understand the human dimensions in flood risk areas, the derived maps and parameters such as buildings, road networks and land use were intersected, and analyzed statistically. Furthermore, the outputs of traditional AHP and the fuzzy AHP method were compared to each other.

The results indicate that the elevation is the most crucial geophysical criteria, while the population parameter is the most significant vulnerability criteria for flood risk assessment for Cedar Rapids. Although AHP and FAHP provide specific differences in the risk level, in general, high- and very-high-risk flood susceptibility zones are primarily found in the downtown areas in both methods. Those areas have lower elevations and are close to the Cedar River. The overall risk level of Cedar Rapids can be stated to be moderate because a risk degree class of 3 has the highest percentage of all maps. Using structures, roads, land use, and population census data from 2010, we provided a summary of vulnerable subgroups into different flood risk zones. We found that the risks with a very low, low, and moderate degree are higher in the AHP method, whereas the percentages in the high and very high fields are higher in the fuzzy method. According to combined flood risk map with the two methods, the results demonstrate that nearly 40% of the population lives in high to very high flood risk zones, with the highest risk group consisting of adults (16-65 ages).

One of the challenges of the study is the creation of pairwise comparison matrices. The literature was used for creating the matrices; however, the weights may be biased due to the locations of the studies in the literature. Governmental institutions may generate standardized and spatially-custom weights for communities to produce more accurate results and support flood mitigation and planning. In addition, newer census information can provide the latest risk. Potentially, new census datasets can be coupled in the analysis as future work. Then, the outputs can be used as a starting point for developing adaptation and mitigation plans to reduce future flood-related losses by water resource specialists, urban planners, engineers, and local governments.

## 5. References


Ahmed, A. I. A., Khan, S., Gani, A., Ab Hamid, S. H., & Guizani, M. (2018, October). Entropy-based fuzzy AHP model for trustworthy service provider selection in the Internet of Things. In *2018 IEEE 43rd Conference on Local Computer Networks (LCN)* (pp. 606-613). IEEE.

Alabbad, Y., Mount, J., Campbell, A. M., & Demir, I. (2021). Assessment of transportation system disruption and accessibility to critical amenities during flooding: Iowa case study. Science of The Total Environment, 148476.

Alabbad, Y., Yildirim, E., & Demir, I. (2022). Flood mitigation data analytics and decision support framework: Iowa Middle Cedar Watershed case study. Science of The Total Environment, 152768.

Boroushaki S, Malczewski J (2010) Using the fuzzy majority approach for GIS-based multicriteria group decision-making. J Comput Geosci 36(3):302–312. doi:10.1016/j.cageo.2009.05.011

Bouamrane, A., Derdous, O., Dahri, N., Tachi, S. E., Boutebba, K., & Bouziane, M. T. (2020). A comparison of the analytical hierarchy process and the fuzzy logic approach for flood susceptibility mapping in a semi-arid ungauged basin (Biskra basin: Algeria). International Journal of River Basin Management, 1-11.

Buchecker, M., Ogasa, D. M., & Maidl, E. (2016). How well do the wider public accept integrated flood risk management? An empirical study in two Swiss Alpine valleys. Environmental Science & Policy, 55, 309-317.

Buckley, J. J. (1985). Fuzzy hierarchical analysis. *Fuzzy sets and systems*, *17*(3), 233-247.

Chang, D. Y. (1996). Applications of the extent analysis method on fuzzy AHP. *European journal of operational research*, *95*(3), 649-655.

Chen SP, Wang RY (2004) Analyzing hazard potential of typhoon damage by applying grey analytic hierarchy process. Nat Hazards 33(1):77–103. doi:10.1023/B:NHAZ.0000035019.39096.b5

Correia, F. N., Da Silva, F. N., & Ramos, I. (1999). Floodplain management in urban developing areas. Part II. GIS-based flood analysis and urban growth modelling. *Water Resources Management*, *13*(1), 23-37.

Dandapat, K., & Panda, G. K. (2017). Flood vulnerability analysis and risk assessment using analytical hierarchy process. *Modeling Earth Systems and Environment*, *3*(4), 1627-1646.

Das, S. (2019). Geospatial mapping of flood susceptibility and hydrogeomorphic response to the floods in Ulhas Basin, India. Remote Sensing Applications: Society and Environment, 14, 60–74. https:// doi.org/10.1016/j.rsase.2019.02.006

Demir, I., Jiang, F., Walker, R. V., Parker, A. K., & Beck, M. B. (2009, October). Information systems and social legitimacy scientific visualization of water quality. In 2009 IEEE International Conference on Systems, Man and Cybernetics (pp. 1067-1072). IEEE.

Demir, I., & Szczepanek, R. (2017). Optimization of river network representation data models for web-based systems. Earth and Space Science, 4(6), 336-347.

Demiray, B. Z., Sit, M., & Demir, I. (2021). D-SRGAN: DEM super-resolution with generative adversarial networks. SN Computer Science, 2(1), 1-11.

Duan, Y., Xiong, J., Cheng, W., Wang, N., Li, Y., He, Y., ... & Yang, G. (2021). Flood vulnerability assessment using the triangular fuzzy number-based analytic hierarchy process and support vector machine model for the Belt and Road region. *Natural Hazards*, 1-26.

Ebert-Uphoff, I., Thompson, D.R., Demir, I., Gel, Y.R., Karpatne, A., Guereque, M., Kumar, V., Cabral-Cano, E. and Smyth, P., (2017), September. A vision for the development of benchmarks to bridge geoscience and data science. In 17th International Workshop on Climate Informatics.

Eini, M., Kaboli, H. S., Rashidian, M., & Hedayat, H. (2020). Hazard and vulnerability in urban flood risk mapping: Machine learning techniques and considering the role of urban districts. International Journal of Disaster Risk Reduction, 50, 101687.

Ekmekçioğlu, Ö., Koc, K., & Özger, M. (2021). District-based flood risk assessment in Istanbul using fuzzy analytical hierarchy process. *Stochastic Environmental Research and Risk Assessment*, *35*(3), 617-637.

Eryılmaz Türkkan, G., & Hırca, T. (2021). The investigation of flood risk perception as a quantitative analysis from a socio-demographic perspective. Natural Hazards, 106(1), 715-733.

Ewing, G., & Demir, I. (2021). An ethical decision-making framework with serious gaming: a smart water case study on flooding. Journal of Hydroinformatics, 23(3), 466-482.

FEMA (2021). FEMA Flood Map Service Center: Hazus. Retrieved from https://msc.fema.gov/portal/resources/hazus

Gautam, A., Sit, M., & Demir, I. (2022). Realistic river image synthesis using deep generative adversarial networks. Frontiers in Water, 4.

Hallegatte, S., A. Vogt-Schilb, M. Bangalore, J. Rozenberg. (2017). Unbreakable: Building the Resilience of the Poor in the Face of Natural Disasters. Climate Change and Development; Washington, DC: World Bank

Haltas, I., Yildirim, E., Oztas, F., & Demir, I. (2021). A comprehensive flood event specification and inventory: 1930–2020 Turkey case study. International Journal of Disaster Risk Reduction, 56, 102086.

Hall, J. W., Meadowcroft, I. C., Sayers, P. B., & Bramley, M. E. (2003). Integrated flood risk management in England and Wales. Natural Hazards Review, 4(3), 126-135.

Hu, A., & Demir, I. (2021). Real-time flood mapping on client-side web systems using hand model. Hydrology, 8(2), 65.

Iowa Department of Natural Resources (DNR) (2021a). Elevation Data. Retrieved from https://www.iowadnr.gov/environmental-protection/air-quality/modeling/dispersion-modeling/elevation-data

Iowa Department of Natural Resources (DNR) (2021b). Iowa Geospatial Data. Retrieved from https://geodata.iowa.gov/documents/iowadnr::stream-centerlines-of-iowa/about

Jones, C.S., Davis, C.A., Drake, C.W., Schilling, K.E., Debionne, S.H., Gilles, D.W., Demir, I. and Weber, L.J., (2018). Iowa statewide stream nitrate load calculated using in situ sensor network. JAWRA Journal of the American Water Resources Association, 54(2), 471-486.

Kerkez, M., Gajović, V., & Puzić, G. (2017). Flood risk assessment model using the fuzzy analytic hierarchy process. *Progress in Economic Sciences*, (4).
Kreibich, H., Di Baldassarre, G., Vorogushyn, S., Aerts, J. C. J. H., Apel, H., Aronica, G. T., Arnbjerg-Nielsen, K., Bouwer, L., Bubeck, P., Caloiero, T., Chinh, D. T., Cortès, M., Gain, A. K., Giampá, V., Kuhlicke, C., Kundzewicz, Z. W., Llasat, C.M., Mård, J., Matczak, P., ... Merz, B. (2017). Adaptation to flood risk: Results of international paired flood event studies. Earth's Future, 5(10), 953–965, https://doi.org/10.1002/2017EF000606
Lei, Y., Wang, J., Yue, Y. et al. Rethinking the relationships of vulnerability, resilience, and adaptation from a disaster risk perspective. Nat Hazards 70, 609–627 (2014). https://doi.org/10.1007/s11069-013-0831-7
Li, Z., & Demir, I. (2022). A comprehensive web-based system for flood inundation map generation and comparative analysis based on height above nearest drainage. Science of The Total Environment, 828, 154420.
Li, Z., Mount, J., & Demir, I. (2022). Accounting for uncertainty in real-time flood inundation mapping using HAND model: Iowa case study. Natural Hazards, 1-28.
Malczewski, J. (1999). GIS and Multi-criteria Decision Analysis, New York: John Willey and Sons.
McClymont, K, Morrison, D., Beevers, L., and Carmen, E. (2020). Flood resilience: a systematic review, J. Environmental Planning and Management, 63(7), pp. 1151-1176, https://doi.org/10.1080/09640568.2019.1641474
Merz, B., Bloschl, G., Vorogushyn, S., Dottori, F., Aerts, J.C.J.H., Pates, P., Berola, M., Kemter, M., Kreibich, H., Lall, U. and Macdonald, E. (2021). Causes, impacts, and patterns of disastrous river floods, Nature Reviews Earth & Environment 2, pp.592-609, https://doi.org/10.1038/s43017-021-00195-3
Meshram, S. G., Alvandi, E., Singh, V. P., & Meshram, C. (2019). Comparison of AHP and fuzzy AHP models for prioritization of watersheds. *Soft Computing*, *23*(24), 13615-13625.
Mikhailov, L. and Tsvetinov, P., 2004. Evaluation of services using a fuzzy analytic hierarchy process. Applied Soft Computing, 5(1), pp.23-33.
Mojaddadi, H., Pradhan, B., Nampak, H., Ahmad, N., & Ghazali, A. H. B. (2017). Ensemble machine-learning-based geospatial approach for flood risk assessment using multi-sensor remote-sensing data and GIS. Geomatics, Natural Hazards, and Risk, 8(2), 1080-1102.
Muste, M., Lyn, D. A., Admiraal, D., Ettema, R., Nikora, V., & García, M. H. (Eds.). (2017). Experimental Hydraulics: Methods, Instrumentation, Data Processing and Management: Volume I: Fundamentals and Methods. CRC Press.
NASS (2021). CroplandCROS, CropScape, and Cropland Data Layer. Retrieved from https://www.nass.usda.gov/Research_and_Science/Cropland/SARS1a.php
OpenStreetMap. (2021) Transportation Network Vector Layer. Retrieved from https://planet.openstreetmap.org
Parhizgar, S. M., Shahidi, A., Pourreza-Bilondi, M., & Khashei-Siuki, A. (2017). Comparison of classic and fuzzy analytic hierarchy processes for mapping the flood hazard of Birjand plain. *Water Harvesting Research*, *2*(1), 43-56.
Proag, V. (2014). The concept of vulnerability and resilience, 4th International Conference on Building Resilience, Building Resilience 2014, 8-10 September 2014, Salford Quays, UK; DOI: 10.1016/S2212-5671(14)00952-6
Putra, D., Sobandi, M., Andryana, S., & Gunaryati, A. (2018). Fuzzy analytical hierarchy process method to determine the quality of gemstones. Advances in Fuzzy Systems, 2018.
Radionovs, A., & Uzhga-Rebrov, O. (2017, June). Comparison of different fuzzy ahp methodologies in risk assessment. In *ENVIRONMENT. TECHNOLOGIES. RESOURCES.*

*Proceedings of the International Scientific and Practical Conference* (Vol. 2, pp. 137-142).
Rentschler, J., & Salhab, M. (2020). People in Harm's Way: Flood Exposure and Poverty in 189 Countries. The World Bank.
Rogers, B. C., Bertram, N., Gersonius, B., Gunn, A., Löwe, R., Murphy, C., ... & Arnbjerg-Nielsen, K. (2020). An interdisciplinary and catchment approach to enhancing urban flood resilience: a Melbourne case. Philosophical Transactions of the Royal Society A, 378(2168), 20190201.
Rufat, S., Tate, E., Burton, C. G., & Maroof, A. S. (2015). Social vulnerability to floods: Review of case studies and implications for measurement. International journal of disaster risk reduction, 14, 470-486.
Saaty, T. L. (1980). The Analytic Hierarchy Process: Planning, Priority Setting, Resource Allocation. United Kingdom: McGraw-Hill International Book Company.
Scheuer, S., Haase, D., & Meyer, V. (2011). Exploring multicriteria flood vulnerability by integrating economic, social, and ecological dimensions of flood risk and coping capacity: from a starting point view towards an end point view of vulnerability. Natural Hazards, 58(2), 731-751.
Sermet, Y., & Demir, I. (2020). Virtual and augmented reality applications for environmental science education and training. New Perspectives on Virtual and Augmented Reality: Finding New Ways to Teach in a Transformed Learning Environment, 261-275.
Sinha R, Bapalu GV, Singh LK, Rath B (2008) Flood risk analysis in the Kosi river basin, north Bihar using multi-parametric approach of analytical hierarchy process (AHP). Indian J Indian Soc Remote Sens 36(4):335–349
Talha, S., Maanan, M., Atika, H., & Rhinane, H. (2019). Prediction of flash flood susceptibility using fuzzy analytical hierarchy process (Fahp) algorithms and Gis: a study case of Guelmim region In Southwestern of Morocco. *The International Archives of Photogrammetry, Remote Sensing and Spatial Information Sciences*, *42*, 407-414.
Tate, E., Strong, A., Kraus, T., & Xiong, H. (2016). Flood recovery and property acquisition in Cedar Rapids, Iowa. Natural Hazards, 80(3), 2055-2079.
Tate, E., Rahman, M. A., Emrich, C. T., & Sampson, C. C. (2021a). Flood exposure and social vulnerability in the United States. Natural Hazards, 106(1), 435-457.
Tate, E., Decker, V., & Just, C. (2021b). Evaluating collaborative readiness for interdisciplinary flood research. Risk analysis, 41(7), 1187-1194.
Teague, A., Sermet, Y., Demir, I. and Muste, M., 2021. A Collaborative Serious Game for Water Resources Planning and Hazard Mitigation. International Journal of Disaster Risk Reduction, 53, p.101977.
Tesfamariam, S., & Sadiq, R. (2006). Risk-based environmental decision-making using fuzzy analytic hierarchy process (F-AHP). *Stochastic Environmental Research and Risk Assessment*, *21*(1), 35-50.
Thieken, A. H., Kienzler, S., Kreibich, H., Kuhlicke, C., Kunz, M., Mühr, B., ... & Schröter, K. (2016). Review of the flood risk management system in Germany after the major flood in 2013. Ecology and Society, 21(2).
Thomas, N. W. (2015). Simulating the hydrologic impact of distributed flood mitigation practices, tile drainage, and terraces in an agricultural catchment. Doctorate Dissertation. The University of Iowa.
U.S. Census Bureau. (2020). Quick Facts. Accessed online: https://www.census.gov/quickfacts/cedarrapidscityiowa Access.
USDA. (2021). Soil Survey Geographic (SSURGO) database. Retrieved from hhttps://www.nrcs.usda.gov/wps/portal/nrcs/detail/soils/survey/?cid=nrcs142p2_053627

UC Drought Management. (2021) Soil Water Holding Characteristics. Accessed online: https://ucanr.edu/sites/UrbanHort/Water_Use_of_Turfgrass_and_Landscape_Plant_Materials/Soil_Water_Holding_Characteristics

Van Laarhoven, P. J., & Pedrycz, W. (1983). A fuzzy extension of Saaty's priority theory. *Fuzzy Sets and Systems*, *11*(1-3), 229-241.

Wang, G., Liu, Y., Hu, Z., Lyu, Y., Zhang, G., Liu, J., ... & Liu, L. (2020a). Flood risk assessment based on fuzzy synthetic evaluation method in the Beijing-Tianjin-Hebei metropolitan area, China. *Sustainability*, *12*(4), 1451.

Wang, W., Zhao, X., Cao, J., Li, H., & Zhang, Q. (2020b). Barriers and requirements to climate change adaptation of mountainous rural communities in developing countries: The case of the eastern Qinghai-Tibetan Plateau of China. Land Use Policy, 95, 104354.

Willet K, Sharda R (1991) Using the analytic hierarchy process in water resource planning: selection of flood control projects. J Scio Econ Plan Sci 25(2):103–112

World Health Organization. (2014). Global report on drowning: preventing a leading killer. Accessed online: https://www.who.int/publications

World Bank. (2021). A Catalogue of Nature-Based Solutions for Urban Resilience. Accessed online: https://openknowledge.worldbank.org/

Yang, W., Xu, K., Lian, J., Bin, L. and Ma, C. (2018). Multiple flood vulnerability assessment approach based on fuzzy comprehensive evaluation method and coordinated development degree model, Journal of Environmental Management, 13, pp. 440-450, https://doi.org/10.1016/j.jenvman.2018.02.085.

Yildirim, E. (2017). Hazus-MH flood loss estimation on a Web-based system. *Master's Thesis*. University of Iowa.

Yildirim, E. & Demir, I., 2019. An integrated web framework for HAZUS-MH flood loss estimation analysis. Natural Hazards, 99(1), pp.275–286.

Yildirim, E., & Demir, I. (2021). An Integrated Flood Risk Assessment and Mitigation Framework: A Case Study for Middle Cedar River Basin, Iowa, US. International Journal of Disaster Risk Reduction, 56, 102113.

Yildirim, E., & Demir, I. (2022a). Agricultural flood vulnerability assessment and risk quantification in Iowa. Science of The Total Environment, 826, 154165.

Yildirim, E., & Demir, I. (2022b). Flood Risk Assessment and Quantification at the Community and Property Level in the State of Iowa. International Journal of Disaster Risk Reduction, 77, 103106.

Zadeh, L. A. (1965). Information and control. *Fuzzy sets*, *8*(3), 338-353.

Zevenbergen, C., Gersonius, B., Radhakrishan, M. (2020) Flood resilience, Phil.Trans. R. Soc. A378, http://dx.doi.org/10.1098/rsta.2019.021